The growth of decagonal Al–Co–Ni single crystals as a function of chemical composition

B. Zhang, M. Estermann, and W. Steurer
Laboratory of Crystallography, ETH Zentrum, CH-8092 Zurich, Switzerland

Decaprismatic single crystals taken from a series of alloys of nominal compositions within $Al_{65-77}Co_{3-22}Ni_{3-22}$ have been studied by means of x-ray diffraction techniques. The substitution of Co by Ni in increasing amounts changes the (pseudo)decagonal diffraction patterns drastically and indicates structural changes which range from a single-crystalline approximant via orientationally ordered nanodomain structures and quasiperiodic phases with different types of ordering phenomena, to a basic decagonal phase. A quantum phase diagram analysis shows a clear separation of the stability regions of the ternary systems described in this study and other decagonal phases.

I. INTRODUCTION

Shortly after the discovery of the first stable decagonal quasicrystals in the ternary systems Al–Co–Cu and Al–Co–Ni,[1] a first systematic investigation of the stability region and the phase equilibria of the decagonal quasicrystal in the system Al–Co–Ni was performed.[2] The stability region of the decagonal phase was found to be within a few atomic percent around the composition $Al_{72}Co_{14}Ni_{14}$ at temperatures between 700 and 1000 °C. Samples of $Al_{70}Co_{15}Ni_{15}$ annealed at 800 °C and at 550 °C show on high-resolution transmission electron microscopic (HRTEM) images the same ring contrasts but with different global ordering. In the high temperature phase they occupy the vertices of a pentagonal tiling and in the low temperature phase those of a rhombic aperiodic tiling with ≈ 20 Å edge length.[3,4] On the corresponding selected area electron diffraction (SAED) photographs, diffuse interlayer lines are observed for the low-temperature phase, indicating a twofold superstructure perpendicular to the quasiperiodic layers. Composition and temperature dependent investigations show a wealth of different diffraction phenomena like superstructure reflections and diffuse scattering corresponding to complicated structural ordering phenomena.[5–9] According to the first x-ray structure analyses on single crystals with nominal compositions $Al_{70}Co_{20}Ni_{10}$ and $Al_{70}Co_{15}Ni_{15}$, respectively, the decagonal phase can geometrically be described by stacking quasiperiodic layers a and A (A denotes the layer a rotated around $\pi/5$) with sequence $...AaAa...$ upon each other.[10,11] The structure building elements, however, are not these layers but columnar clusters with ≈ 20 Å diameter and helical symmetry $10_5/mmc$ that correspond to the ring contrasts observed by HRTEM.[3,4,9] It was observed that decagonal $Al_{70}Co_{15}Ni_{15}$ transforms during electron-beam irradiation in the electron microscope into two different quasiperiodic superstructures:

one of them is characterized by the typical ≈ 20 Å ring contrasts, the other by ≈ 6 Å circular patterns.[9]

Despite the large amount of experimental work already done on the Al–Co–Ni system, many questions are yet to be answered: Does a perfectly ordered decagonal phase (without any diffuse scattering) exist, and in which compositional and temperature range is it stable? What happens structurally as a function of the Co/Ni ratio? Which superstructures and/or modulated structures of the decagonal phase are stable? What approximant phase does the decagonal phase transform to? Another important problem is the growth of as perfect as possible single crystals of decagonal Al–Co–Ni for structural investigations and for the study of physical properties. Consequently, one of the goals of the present work was to find the optimum sample compositions for growing large idiomorphous single crystals of the decagonal phase by slowly cooling from the melt.

II. EXPERIMENTAL

A series of Al–Co–Ni alloys with different compositions was prepared by melting compacts of mixtures of the high-purity elements (Heraeus, Al: 99.99%; Co: 99.99%; Ni: 99.99%) in an induction furnace under argon (PanGas, 99.998%) atmosphere. After remelting the prealloys in a high-vacuum furnace (PVA, $\approx 1 \times 10^{-4}$ Pa), the samples were slowly cooled at rates of $0.5-1$ Kmin^{-1} to 1073 K and subsequently quenched by jetting argon in the sample chamber of the switched-off furnace. The ingots were crushed and single crystals with $0.1-0.3$ mm diameter and up to ≈ 0.5 mm length were selected for the x-ray diffraction experiments. From all samples, x-ray precession photographs were taken using Mo K$_\alpha$ radiation. The photographs with tenfold symmetry with $F = 100$ mm crystal film distance and precession angle $\mu = 17°$, on an 18 KW Siemens rotating-anode generator, were equipped with (virtual)

0.3×0.3 mm fine focus and graphite monochromator, and the other photographs ($F = 60$, $\mu = 30°$) on a fine-focus x-ray tube with Johansson-type focusing quartz-monochromator. Exposure times covered 28 h to 163 h depending on the crystal size. The chemical compositions of the samples were determined with an accuracy of ≈ 0.1 at. % by electron microprobe analysis (CAMECA SX50), and their microstructure was inspected by optical polarization microscopy. According to the results of the electron microprobe analyses, the compositions of the samples are all within the range of $Al_{70.6–73.5}(Co, Ni)_{29.4–26.5}$, indicating a nearly constant Al to transition metal (TM) ratio.

III. RESULTS

The photomicrographs and x-ray precession photographs of five of the seven Al–Co–Ni alloys studied are shown in Figs. 1–5. Their starting compositions are marked b, c, d, e, g in Fig. 6. The indexing of the precession photographs refers to a reciprocal basis[11] with $a_i^* = 0.2636$ Å^{-1}, $i = 1 \ldots 4$, and $a_5^* = 0.24506$ Å^{-1}. This is related to a quasilattice constant (edge length of the Penrose rhomb) of $a_r = 2\tau/(5a^*) = 2.456$ Å with $\tau = (1 + 5^{1/2})/2$. The white pentagram constructions on the tenfold precession photographs are to help distinguish fundamental quasicrystal reflections (only on line intersections) from superstructure phenomena. On the photographs also a number of reflections are indexed to allow an unambiguous interpretation and discussion. It is obvious that the diffraction patterns change gradually from the crystalline structure (not shown here) to an almost perfect quasicrystal structure when the Ni content is raised. The nominal sample compositions and those of the phases formed during thermal treatment are illustrated in a ternary concentration diagram (Fig. 6). The typical growth morphology of both twinned approximant and single crystalline decagonal phase is shown in Fig. 7. Decaprismatic needles are formed in both cases, but the grains grow much bigger in the case of the approximant.

The Ni poor end member $Al_{13-x}(Co_{1-y}Ni_y)_4$, with $x = 0.9$, $y = 0.12$ (composition marked a in Fig. 6), is an approximant of the decagonal quasicrystal with monoclinic structure isotypic to that of $Al_{13}Os_4$.[12] Substituting a few atomic percent Co by Ni (composition marked b in Fig. 6), a single-phase alloy is obtained with large decaprismatic crystals (Fig. 7). On a first glance, one could mistake its diffraction pattern (Fig. 1) for that of a decagonal quasicrystal. A detailed analysis, however, shows splitting of particular reflections, one of them is marked by an arrow in Fig. 1(b), typical for a structure with crystalline nanodomains arranged in five allowed orientations [Fig. 8(a)]. It cannot be excluded, however, that beside the approximant domains also a quasiperiodic

average structure exists. This can be decided only by high-resolution x-ray experiments.[13,14]

A further increase of the Ni content (composition marked c in Fig. 6) leads to a two-phase alloy of decagonal phase and $Al_4(Co, Ni)_3$, and subsequently to a single-phase sample (composition marked d in Fig. 6). The precession photographs (Figs. 2 and 3) of the decagonal phases in the two samples show sharp Bragg spots surrounded by two types of satellite reflections [marked in
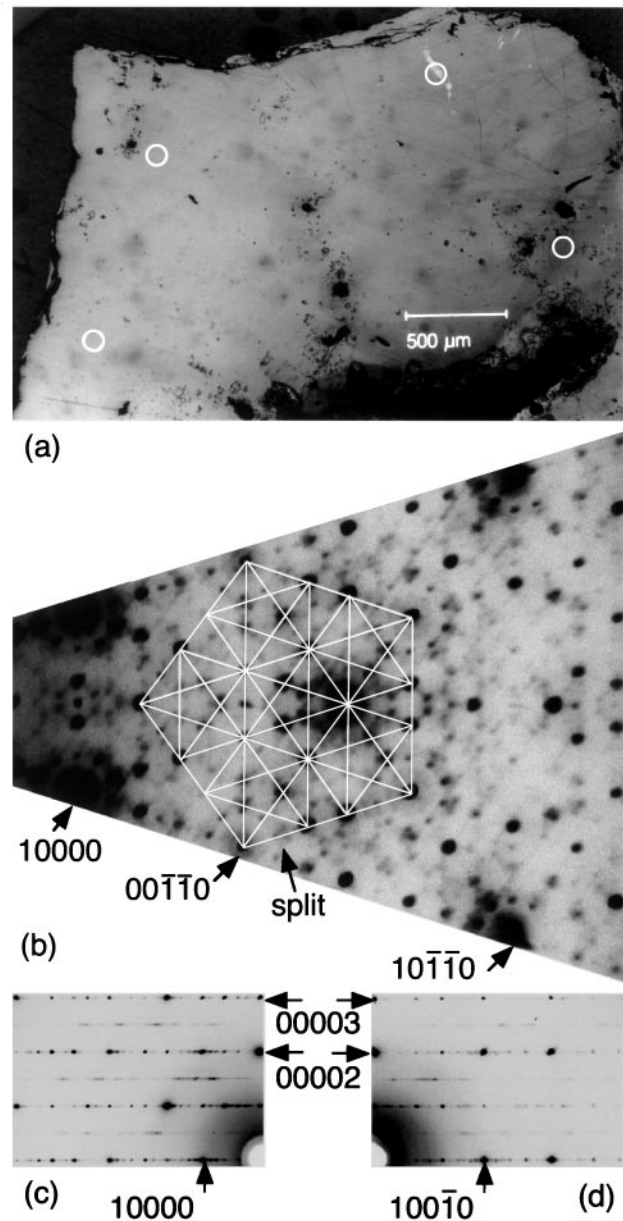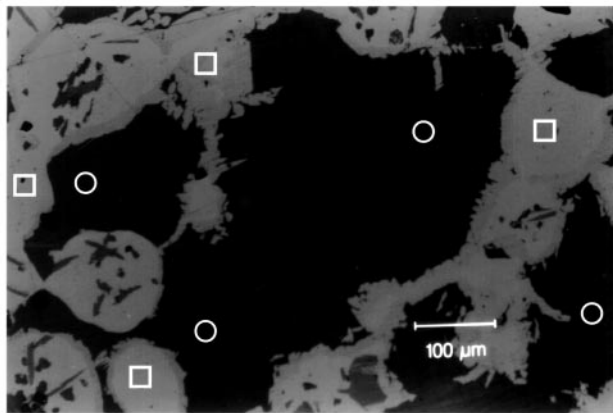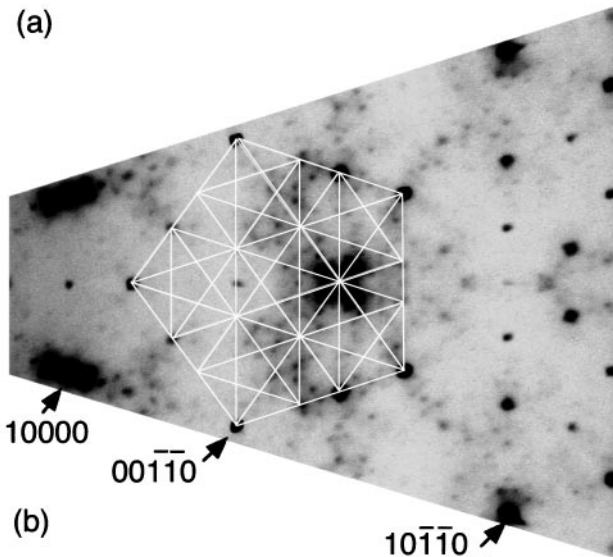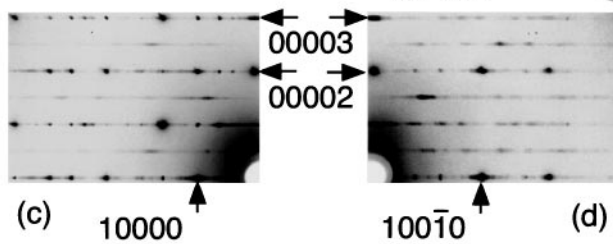

FIG. 1. (a) Photomicrograph (polarized light) of an alloy with nominal composition $Al_{75}Co_{20}Ni_5$ (marked b in Fig. 6). The composition was determined by microprobe analysis to $Al_{73.5}Co_{21.7}Ni_{4.8}$ at the points marked (○). (b) Tenfold and twofold, (c) D-, and (d) P-direction x-ray precession photographs. One typical split position is marked by an arrow in (b) (compare also Fig. 8).
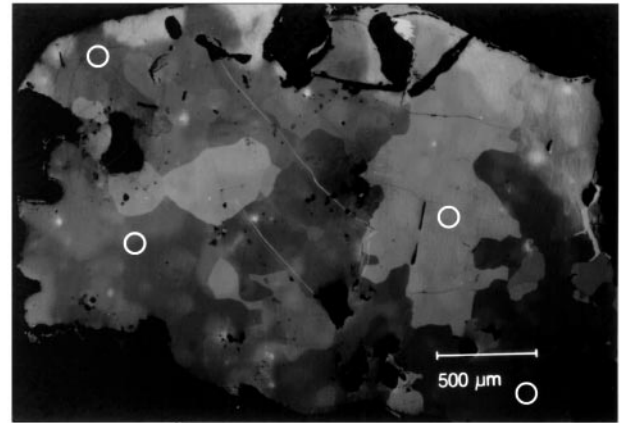
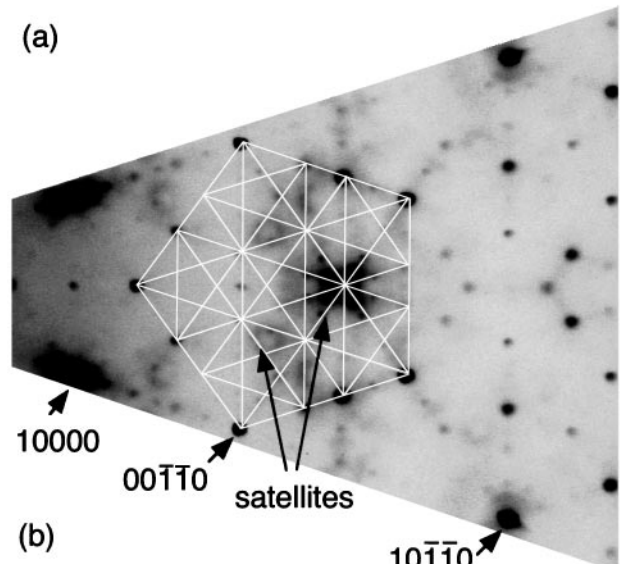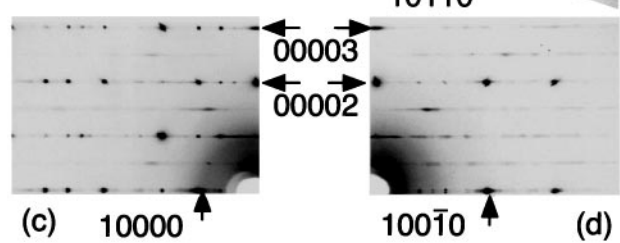FIG. 2. (a) Photomicrograph (polarized light) of the alloy with nominal composition $Al_{65}Co_{20}Ni_{15}$ (marked c in Fig. 6). The composition was determined by microprobe analysis to $Al_{70.7}Co_{19.0}Ni_{10.3}$ at the points marked (○) and to $Al_{57.0}Co_{23.1}Ni_{19.9}$ at the points marked (□). (b) Tenfold and twofold, (c) D-, and (d) P-direction x-ray precession photographs taken from a crystal with composition $Al_{70.7}Co_{19.0}Ni_{10.3}$.

FIG. 3. (a) Photomicrograph (polarized light) of the alloy with nominal composition $Al_{77}Co_{15}Ni_8$ (marked d in Fig. 6). The composition was determined by microprobe analysis to $Al_{71.0}Co_{17.7}Ni_{11.3}$ at the points marked (○). (b) Tenfold and twofold, (c) D-, and (d) P-direction x-ray precession photographs taken. The two types of satellite reflections are marked by arrows in (b).

Fig. 3(b)] and structured diffuse scattering. It was found by high-resolution x-ray diffraction that the satellites around the main reflections occupy positions belonging to the reciprocal lattices of the twinned approximant[14]; this may also be true for the other type of satellites occurring in groups of five on the corners of small pentagons. From low resolution SAED experiments, these satellites were interpreted to correspond to a twofold superstructure of the quasiperiodic phase.[9] Again, a high-

resolution measurement is needed to find the correct assignment.

By increasing further the Ni content (composition marked e in Fig. 6), diffraction patterns are obtained with the positions of main reflections unchanged, but sharp superstructure reflections around the Bragg spots replace the previous smeared diffuse scattering phenomena (Fig. 4). These superstructure reflections, which are located in centers of pentagonally arranged main
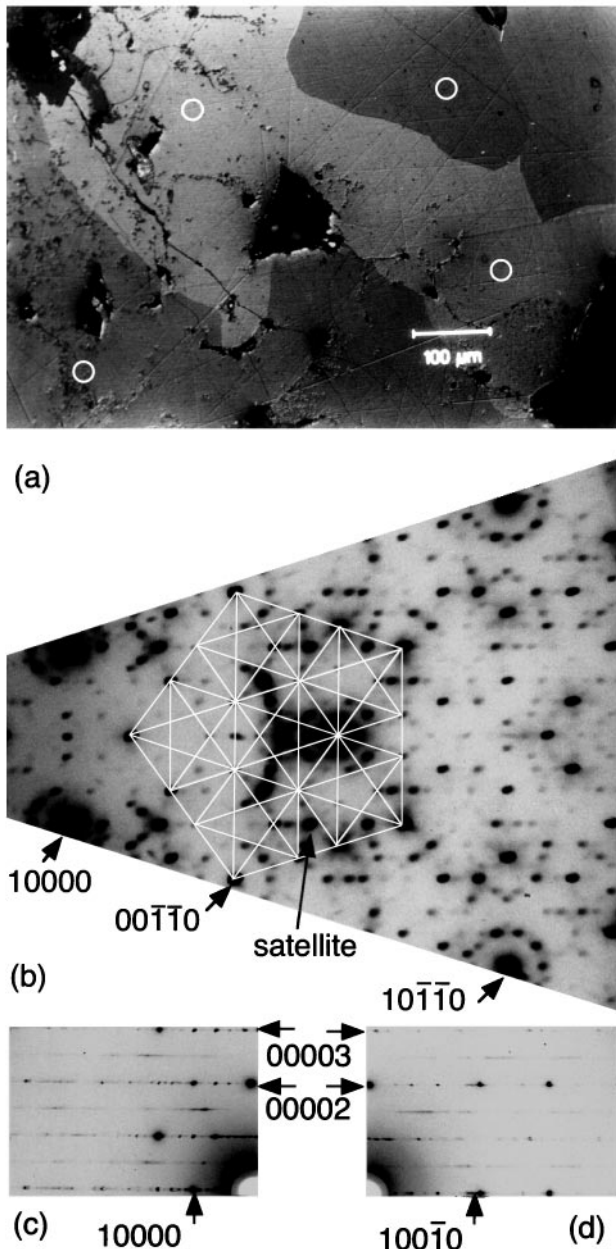
FIG. 4. (a) Photomicrograph (polarized light) of the alloy with nominal composition $Al_{75}Co_{10}Ni_{15}$ (marked e in Fig. 6). The composition was determined by microprobe analysis to $Al_{72.7}Co_{11.6}Ni_{15.7}$ at the points marked (○). (b) Tenfold and twofold, (c) D-, and (d) P-direction x-ray precession photographs. The type S1 satellite is marked by an arrow in (b).

FIG. 5. (a) Photomicrograph (polarized light) of the alloy with nominal composition $Al_{75}Co_3Ni_{22}$ (marked g in Fig. 6). The composition was determined by microprobe analysis to $Al_{70.6}Co_{6.8}Ni_{22.6}$ at the points marked (○), to $Al_{82.6}Co_{3.8}Ni_{13.7}$ at the points marked (□), and to $Al_{62.7}Co_{2.7}Ni_{34.6}$ at the points marked (★). (b) Tenfold and twofold, (c) D-, and (d) P-direction x-ray precession photographs taken from a crystal with composition $Al_{70.6}Co_{6.8}Ni_{22.6}$. The diffuse reflection present in all precession photographs located halfway between the $00\bar{1}\bar{1}0$ reflection and its symmetrically equivalent one is a higher harmonic ($\lambda/2$).

reflections [marked in Fig. 4(b)], can be identified as the type S1 reflections described elsewhere.[5–7] Finally, at very high Ni content (compositions marked f and g in Fig. 6), these satellite reflections become diffuse and disappear eventually (Fig. 5).

The x-ray diffraction patterns along the two inequivalent twofold directions, i.e., the reciprocal lattice rods running along (D-direction) and between
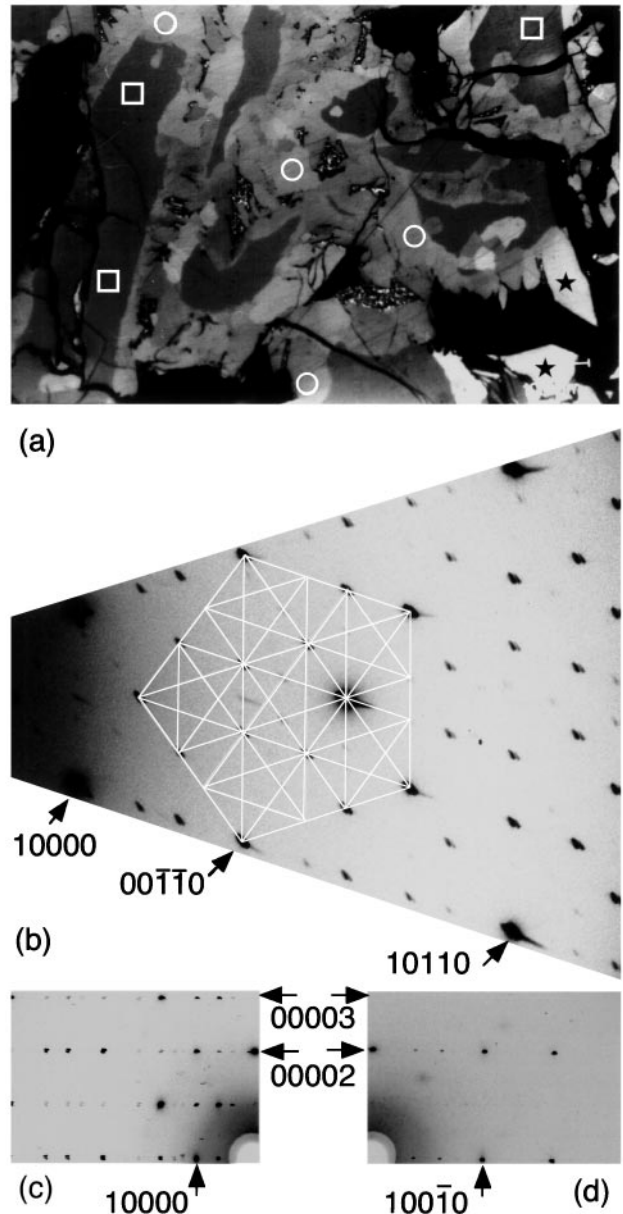
(P-direction) the reciprocal basis vectors $\mathbf{a}_i^*, i = 1 \ldots 4$, respectively, are also shown in Figs. 1–5. With increasing Ni content the diffuse intensities within the Bragg layers (corresponding to the ≈ 4 Å period) and the interlayers (≈ 8 Å superperiod) diminish gradually until they disappear completely. In a similar way

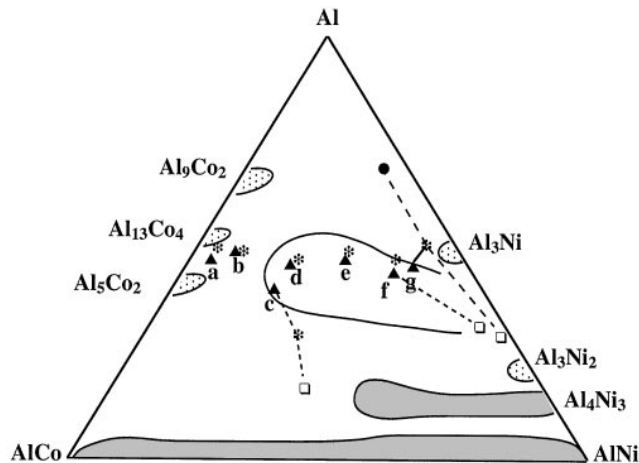J. Mater. Res., Vol. 12, No. 9, Sep 1997

2277

FIG. 6. Concentration diagram of Al–Co–Ni alloys. Compositions of compacts are marked by stars; compositions of phases found in annealed samples are marked by triangles in the case of decaprismatic single crystals and by squares and full circles in the other cases. Phases discussed in the text are marked by letters a . . . g. The range of formation of decagonal phases is qualitatively indicated by the solid line.

the reflections $(0\ 0\ 0\ 0\ h_5)$: $h_5 = 2n + 1$, marked by arrows on the P-direction x-ray photographs, become gradually more diffuse and cannot be observed any more in Figs. 4 and 5. On the P-direction x-ray photographs the behavior of the $(h_1 h_2 \overline{h}_2 \overline{h}_1 h_5)$: $h_5 = 2n + 1$ reflections is also demonstrated as a function of the Ni concentration. The absence of these two reflection classes in reciprocal space is equivalent to a 10_5-screw axis and a c-glide plane in the five-dimensional direct space which is typically used for structure description.[11]

IV. DISCUSSION

The interpretation of the x-ray precession photographs (Figs. 1–5) shows that the stability region of the decagonal phase has to be extended to much lower Co concentrations than previously assumed.[2,8] Even more, the best ordered decagonal phase, i.e., that with the least diffuse scattering, has a similar composition as the closely related decagonal phase in the Al–Fe–Ni system,[8] i.e., $Al_{70.6}Co_{6.8}Ni_{22.6}$ compared to $Al_{71.5}Fe_5Ni_{23.5}$. Substitution of Ni by Co causes ordering processes within the quasiperiodic layers and also a doubling of the translation period perpendicular to them. Since the interlayer lines on the type D and P x-ray and SAED photographs remain diffuse even after very long annealing times,[8] the quasiperiodic superstructure is less perfect than its fundamental structure. The satellite reflections and the diffuse scattering in the Bragg layers of the samples with Co/Ni ratio approximately equal to one indicate larger deviations from a quasiperiodic ordering of the structure-building elements. In these samples, as we know from HRTEM investigations,[3,4,9]
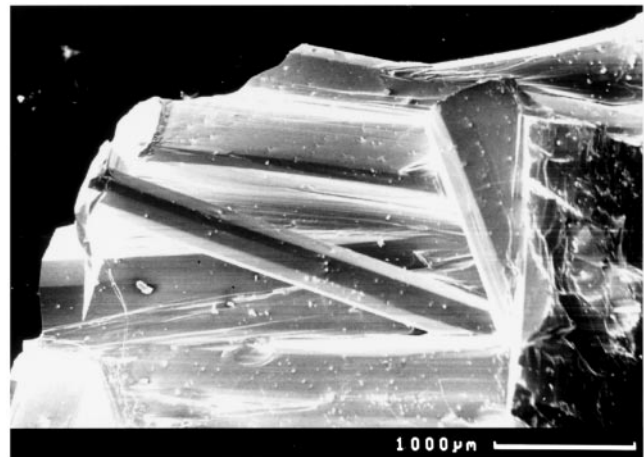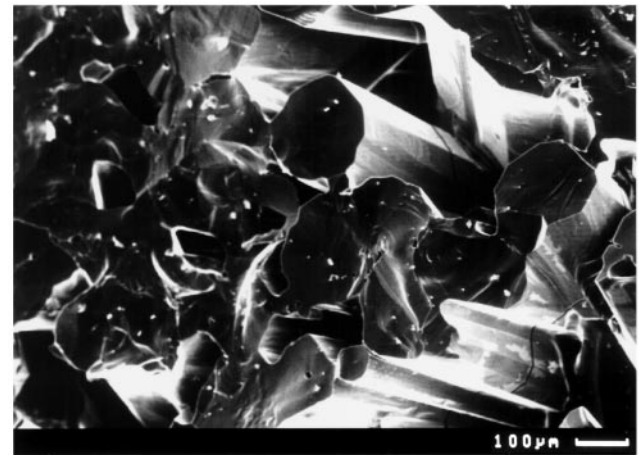
FIG. 7. Scanning electron microscope (SEM) images of (a) the twinned approximant $Al_{73.5}Co_{21.7}Ni_{4.8}$ (marked b in Fig. 6) and (b) the decagonal phase $Al_{71.0}Co_{17.7}Ni_{11.3}$ (marked d in Fig. 6), demonstrating the typical growth morphology.

nanodomain structures are formed. Depending on their domain size distribution function, their diffraction patterns consist of contributions from coherently scattering domains with globally quasiperiodic phase relationships at the domain boundaries, and also of contributions from individual domains with statistical phase relationships at the domain boundaries.

The role of the Co/Ni ratio as structure directing parameter in the decagonal Al–Co–Ni system will be discussed in the following paragraph. Several attempts have already been made to explain and predict the conditions for the existence of stable decagonal (or icosahedral) quasicrystals. An often used criterion is the average valence electron concentration per atom e/a. It was found that for many quasiperiodic phases this ratio adopts values between 1.7 and 1.8.[1] The
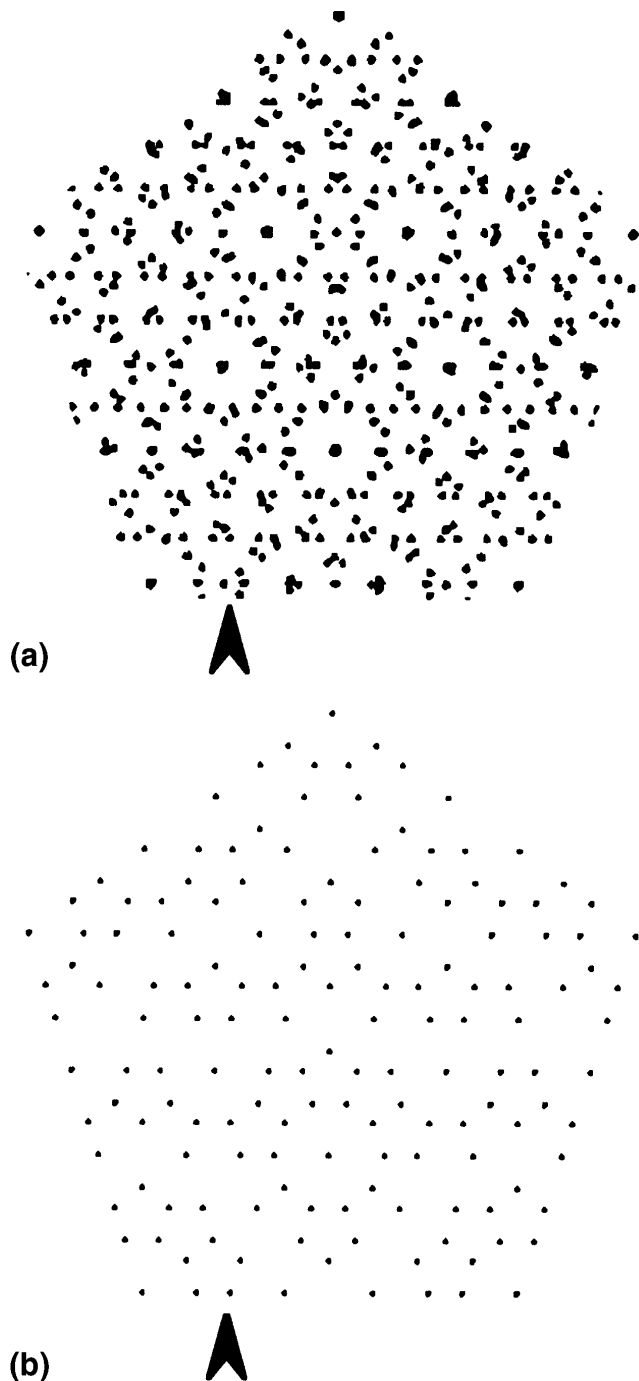
(a)

(b)

FIG. 8. Calculated zero-layer x-ray diffraction patterns (a) of an incoherently fivefold twinned c-centered orthorhombic approximant with $a = 61.024$ Å and $b = 83.99$ Å, and (b) of a quasicrystal with edge length $a_r = 2.456$ Å of Penrose rhombs. The split reflection marked in Fig. 1(b) is also marked in (a) by an arrowhead.
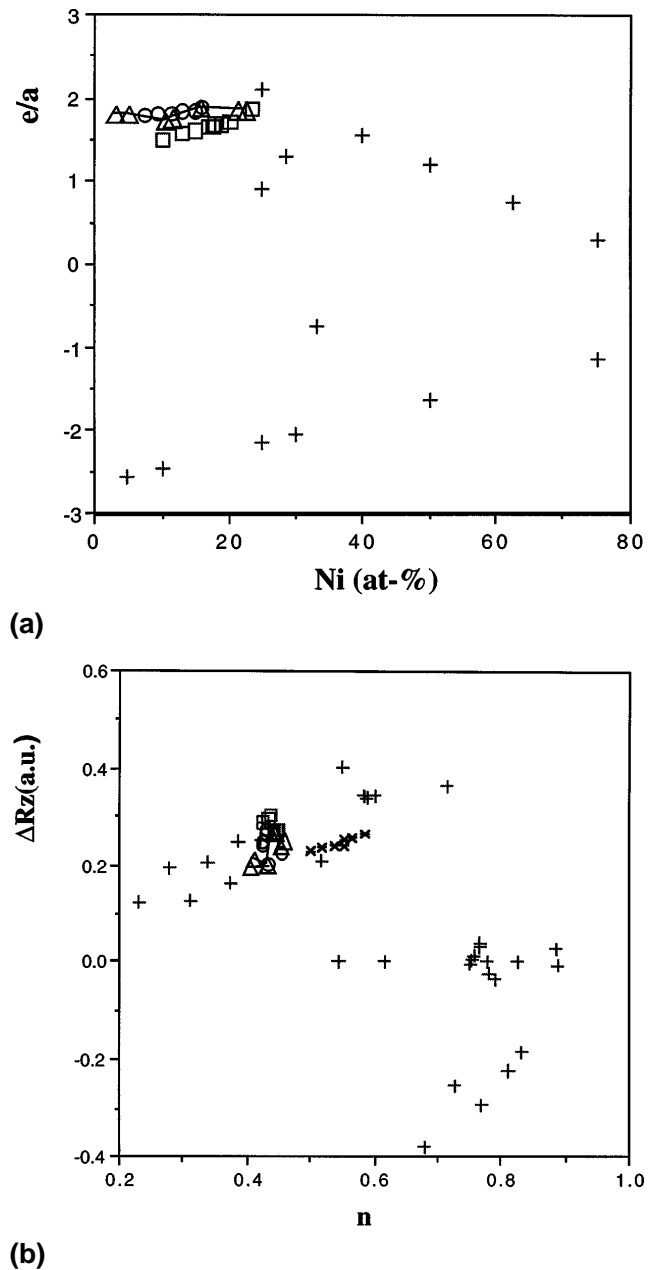

(a)

(b)

FIG. 9. The relationship between the Ni contents and (a) the average outer electron per atom ratio (e/a); (b) the weighted Zunger's pseudo-potential core radius ΔRz as a function of n, the ratio of the number of $3d$ valence electrons to the total number of valence electrons in the compound. The open triangles (connected by a line) correspond, from left to the right, to the samples a . . . g and decagonal Al–Fe–Ni, the circles and squares to the decagonal Al–Co–Ni and Al–Co–Cu samples, respectively, discussed by Grushko,[8] and the crosses denote binary and ternary crystalline compounds in the systems Al–Co–Ni, Al–Fe–Ni in (a), and additionally Al–Co–Cu in (b).

variation of e/a as a function of the Ni concentration is illustrated in Fig. 9(a). The e/a values used are those reported by Raynor[15]: Al + 3, Co − 1.71, Fe − 2.66, Ni − 0.61, and it was supposed that these values do not change with changing Co/Ni ratio. It is obvious

that all samples studied and decagonal Al–Fe–Ni have nearly identical e/a values, $e/a \approx 1.85$. All other Ni-containing binary and ternary phases in the systems Al–Co–Ni and Al–Fe–Ni but Al$_3$Ni exhibit clearly different values.

There are further parameters that have been used successfully in order to systematize the relationships between composition and structure within the quantum structural diagram (QSD) technique, the Zunger pseudopotential core radius R_Z, the Martynov–Batsanov electronegativity X_{MB},[16–20] and the for transition metals important ratio of the number n of $3d$ valence electrons to the total number of valence electrons in the compound. For ternary alloys with composition $A_x B_y C_z$ ($x \leqslant y \leqslant z$ and $x + y + z = 1$), the concentration-weighted variables are defined as follows:

$$\Delta X_{MB} = 2x(X_{MB(A)} - X_{MB(B)}) + 2x(X_{MB(A)} - X_{MB(C)}) + 2y(X_{MB(B)} - X_{MB(C)}),$$

$$\Delta R_z = 2x(R_{z(A)} - R_{z(B)}) + 2x(R_{z(A)} - R_{z(C)}) + 2y(R_{z(B)} - R_{z(C)}),$$

$$n = (x N_{3d(A)} + y N_{3d(B)} + z N_{3d(C)}) / (x N_{(A)} + y N_{(B)} + z N_{(C)}),$$

where $N_{3d(A)}$, $N_{3d(B)}$, and $N_{3d(C)}$ are the numbers of the $3d$ valence electrons and $N_{(A)}$, $N_{(B)}$, and $N_{(C)}$ are all the valence electrons of elements A, B, and C, respectively. In Fig. 9(b) the variation of ΔR_z (ΔX_{MB} shows no unique behavior) is illustrated as a function of n for the samples a . . . g, and of the compounds existing in the related ternary systems Al–Fe–Ni and Al–Co–Cu. It is remarkable that the decagonal phases and their close approximants cluster together around $\Delta R_z \approx 0.25$ and $0.4 \leqslant n \leqslant 0.6$.

V. CONCLUSIONS

X-ray precession photographs of a series of samples with compositions ranging from $Al_{73.9}Co_{23.3}Ni_{2.9}$ to $Al_{70.6}Co_{6.8}Ni_{22.6}$ show a decisive influence of the Co/Ni ratio on the formation of well-ordered decagonal quasicrystals. On the Co-rich side of the phase diagram, there exist stable approximants of the decagonal phase like $Al_{13}Co_4$ and $Al_{13-x}(Co_{1-y}Ni_y)_4$ with $x = 0.9$, $y = 0.12$, respectively. This hinders the formation of the quasiperiodic phase, and supports the growth of

nanodomain structures and superstructures along the periodic direction. In quantum structure diagrams the stability regions of the decagonal phase appear clearly separated from those of the crystalline compounds.

REFERENCES

1. A. P. Tsai, A. Inoue, and T. Masumoto, Mater. Trans. JIM **30**, 463 (1989).
2. S. Kek, Thesis, University of Stuttgart, Germany (1991).
3. K. Hiraga, F. J. Lincoln, and W. Sun, Mater. Trans. JIM **32**, 308 (1991).
4. K. Hiraga, W. Sun, and A. Yamamoto, Mater. Trans. JIM **35**, 657 (1994).
5. K. Edagawa, M. Ichihara, K. Suzuki, and S. Takeuchi, Philos. Mag. Lett. **66**, 19 (1992).
6. K. Edagawa, H. Sawa, and S. Takeuchi, Philos. Mag. Lett. **69**, 227 (1994).
7. K. Edagawa, H. Tamaru, S. Yamaguchi, K. Suzuki, and S. Takeuchi, Phys. Rev. B **50**, 12 413 (1994).
8. B. Grushko and K. Urban, Philos. Mag. B **70**, 1063 (1994).
9. S. Ritsch, C. Beeli, H-U. Nissen, and R. Lück, Philos. Mag. A **71**, 671 (1995).
10. A. Yamamoto, K. Kato, T. Shibuya, and S. Takeuchi, Phys. Rev. Lett. **65**, 1603 (1990).
11. W. Steurer, T. Haibach, B. Zhang, S. Kek, and R. Lück, Acta Crystallogr. B **49**, 661 (1993).
12. B. Zhang, V. Gramlich, and W. Steurer, Z. Kristallogr. **210**, 498 (1995).
13. M. Kalning, S. Kek, B. Burandt, W. Press, and W. Steurer, J. Phys.: Cond. Mat. **6**, 6177 (1994).
14. M. Kalning, W. Press, and S. Kek, Philos. Mag. Lett. **71**, 341 (1995).
15. G. V. Raynor, Progress Metal Physics **1**, 1 (1949).
16. K. M. Rabe, J. Alloys and Compounds **197**, 131 (1993).
17. K. M. Rabe, A. R. Kortan, J. C. Phillips, and P. Villars, Phys. Rev. B **43**, 6280 (1991).
18. K. M. Rabe, J. C. Phillips, P. Villars, and I. D. Brown, Phys. Rev. B **45**, 7650 (1992).
19. J. Tartas, and E. J. Knystautas, J. Mater. Res. **6**, 1219 (1991).
20. P. Villars and F. J. Hulliger, J. Less-Com. Met. **132**, 289 (1987).